Environmental Science and Pollution Research (2018) 25:16913–16921
https://doi.org/10.1007/s11356-018-1878-5

RESEARCH ARTICLE

Reduction mechanism of hexavalent chromium by functional groups of undissolved humic acid and humin fractions of typical black soil from Northeast China

Jia Zhang[1] · Huilin Yin[1] · Hui Wang[1] · Lin Xu[1] · Barnie Samuel[1] · Fei Liu[1] · Honghan Chen[1]

Received: 30 October 2017 / Accepted: 26 March 2018 / Published online: 5 April 2018

Abstract
Soil organic matters (SOM) have a great retention effect on Cr(VI) migration in subsurface environment, which act as the main electron donors for Cr(VI) reduction; however, Cr(VI) reduction mechanism by different SOM fractions is still unclear, such as undissolved humic acid (HA) and humin (HM). In this study, HA and HM fractions extracted from typical black soil from Northeast China were used to investigate the reaction mechanism between humus functional groups and Cr(VI). According to the results, phenol and hydroxyl were determined as the main electron donors for Cr(VI) reduction by HA and HM instead of carboxyl and carbonyl, which were more likely involved in Cr complexation. Furthermore, Cr(VI) reduction was more dependent on aromatic carbon, rather than aliphatic carbon, and functional groups on the particle surfaces of HA and HM were much more active for Cr(VI) reduction than their interior part. Additionally, HM was found to have a relatively low Cr(VI) reduction capability compared with HA resulting from its high content of cellulose structures that are quite resistant to Cr(VI) oxidation. These results suggest that in the soil environment, undissolved HA tends to play a much more important role than HM in Cr(VI) reduction and retention in the condition that their mass contents are comparable.

Keywords Humic acid · Humin · Functional groups · Hexavalent chromium · Reduction

Introduction

Chromium is widely used in the industry, such as electroplating, leather tanning, and dyeing. Unsuitable storage and improper disposal of the leakage have led to many instances where chromium is released into subsurface environment, and this has made chromium become one of the most common heavy metal pollutants in soil and groundwater (Dhal et al. 2013; Hsu et al. 2010; Wittbrodt and Palmer 1996). Compared with other heavy metals, chromium chemistry is more complex, because it cannot only exist in various oxidation states, but also able to exist as anions and cations (Raddatz et al. 2011). In natural environment, Cr(VI) is mainly generated from anthropogenic activities, and it exists as various species of anions under different pH conditions, such as $Cr_2O_7^{2-}$, $HCrO_4^-$, and CrO_4^{2-}, which are all of high mobility and strong toxicity to human (Nickens et al. 2010). On the contrary, Cr(III) exists as cations, such as Cr^{3+}, $Cr(OH)^{2+}$, and $Cr(OH)_2^+$, that are readily adsorbed onto negatively charged sediment particles, and Cr(III) is the essential trace element needed by human body, the toxicity of which is at least two magnitude lower than that of Cr(VI) (Brose and James 2010; Kožuh et al. 2000). Therefore, the reduction of Cr(VI) to Cr(III) is regarded as the most crucial natural process to reduce the environmental risk of chromium by decreasing its mobility and toxicity (Fendorf 1995; Jardine et al. 1999; Kimbrough et al. 1999).

Generally, soil layer has a great retention effect on the migration of Cr(VI) infiltrating from surface, and the existences of soil organic matter (SOM), Fe(II), and S(II) are considered to be responsible for this process. They act as main electron donors for Cr(VI) reduction, and then, the generated Cr(III) is much more readily adsorbed or precipitated on soil particles (Hsu et al. 2009). However, Fe(II) and S(II) are very unstable under oxic soil condition, and thus, SOM is considered to play

Responsible editor: Zhihong Xu

✉ Fei Liu
feiliu@cugb.edu.cn

[1] Beijing Key Laboratory of Water Resources and Environmental Engineering, China University of Geosciences, Beijing 100083, People's Republic of China

the most important role for the reduction of Cr(VI) in the soil environment (Al-Abadleh et al. 2005). Even though much work so far has focused on the relationship between SOM and Cr(VI) reduction and adsorption, considering that SOM is of high chemical heterogeneity that can be classified into humic acid (HA), fulvic acid (FA), and humin (HM) according to their solubility in alkaline and acidic solutions (Van and Comans 2007; Zhang et al. 2013); it is of great scientific significance to reveal the reaction mechanism between Cr(VI) and various SOM fractions. Particularly, HM has been reported to play a much more important role compared with HA in polycyclic aromatic hydrocarbons (PAHs) sorption (Bonin and Simpson 2007; Tang et al. 2008; Zhang et al. 2009a), and it is widespread in soil matrix and contributes to more than 50% of organic carbon in soils (Simpson et al. 2007; Watanabe and Kuwatsuka 1991). However, to our knowledge, there are few studies devoted to interaction between Cr(VI) and HM, especially the effect of differences between HA and HM from a single soil sample.

Undissolved HA and HM are the major constituents of SOM with quite different properties (Zhang et al. 2009b). HA has a high content of polar functional groups, such as aromatic carboxyl groups, phenols and hydroxyls, while HM has much higher molecular weight with higher percentage of aliphatic structures and apolar functional groups, such as carbonyl, esters, and ethers (Yang et al. 2011). The essential process of Cr(VI) reduction by SOM is the oxidation of reductive organic functional groups (Zhang et al. 2017a, 2018), and thus, we can hypothesize that the differences in functional groups and molecular structure between HA and HM would induce dissimilar reduction mechanism for Cr(VI). Therefore, it is of great importance to reveal the mechanism between Cr(VI) and various SOM fractions, which will help better understand the impact of each individual component of soil on Cr(VI) fate in the environment.

In this work, HA and HM were extracted from a typical black soil (corresponding to Mollisol soil according to USDA soil classification system) collected from Northeast China, which is one of the three most important black soil regions worldwide. Compared with the other two black soil regions (the great plains of Ukraine and the Mississippi River basin of America), the black soil region in Northeast China is quite different in the vegetation form, types of parent rock, temperature, precipitation, and geomorphic features, which may lead to various characterizations of humus in the black soil under different humification conditions. At present, the International Humic Substances Society (IHSS) only supplies standard humic acid and fulvic acid extracted from the Elliott soil collected from Mississippi River basin and reference ones extracted from soil collected from Summit Hill of New Zealand, but there are still no available standard or reference humic acid, fulvic acid, or humin extracted from typical black soil in Northeast Asia. Consequently, the extraction of humus fractions from typical black soil in Northeast China and studying their environmental features will benefit the understanding of environmental processes of various pollutants influenced by soil humus in this area and promote the comparisons of molecular characterizations and environmental implications between humic substances from various black soil regions. In addition, the utilization of HA and HM from a single soil sample was aimed to eliminate the effect of various minerals, precursors of SOM, and other factors on Cr(VI) reduction.

It should be emphasized that the HA mentioned in this paper mainly refers to its undissolved form, the content of which is generally two magnitude higher than that of dissolved HA in soil matrix (Xiao et al. 2012), and thus, the undissolved HA is suggested to play a far more important role in the reduction and retention of Cr(VI) compared with dissolved HA in subsurface environment. Additionally, the preliminary experiment was conducted under pH ranging from 1.0 to 5.0, and it was found that the lower pH was beneficial for the retention of Cr(VI) by HA. Therefore, in order to get the results within an acceptable time scale and make HA maintain its undissolved form, we mainly presented the results obtained at pH 1.0. This situation is equally common in contaminated sites associated with electroplating and leather tanning industries (Dermentzis et al. 2011; Liu et al. 2011), where the extremely acidic wastewater (pH 1.0) discharged into the environment directly or by the means of seepage pits have been reported in many sites (Hsu et al. 2007). The objectives of this study were to (1) investigate the differences on functional groups and molecular structures between undissolved HA and HM fractions of typical black soil sample from Northeast China, (2) determine Cr(VI) reduction processes by HA and HM, and (3) reveal the mechanism of HA and HM functional groups for Cr(VI) reduction.

Materials and methods

Soil sample source

The black soil sample was obtained from an undisturbed area at the valley to the southwest of Daqiao Township, Dunhua, Jilin Province (43°19′15″N, 128°21′17″E). The black soil consists of very deep, somewhat poorly drained soils on basalts. Mean annual precipitation is about 645.8 mm, and mean annual air temperature is about 2.1 °C. The plants in the region are mainly of mixed deciduous coniferous broad-leaved forest, and meadow vegetation exists as well. The soil sample was collected from the surface layer within the depth of 30 cm, and then naturally air-dried, ground to homogeneous, passed through a 100-mesh sieve, and stored in sealed brown glass bottles before treatment. The chemical composition, organic matter content, and pH are summarized in Table 1.

Table 1 Chemical composition, organic matter content, and pH of the soil sample

Chemical composition (%)					OM (%)[a]	pH_{KCl}[b]
SiO_2	Al_2O_3	Fe_2O_3	K_2O	CaO		
47.32	16.46	5.57	2.73	1.21	19.36	3.55

[a] The content of organic matter was determined by Walkley-Black procedure

[b] The pH value was measured at soil to 1 M KCl solution ratio of 1:2.5 (*w*/*v*)

Extraction and characterization of HA and HM

The extraction of HA and HM refers to the recommended method by IHSS with minor modification. Briefly, a certain amount of soil sample was shaken for 24 h at 50 °C with 0.1 M $Na_4P_2O_7$/0.1 M NaOH solution with soil to solution ratio of 1:10 (*w*/*v*), and the air in the bottle was replaced with N_2. Subsequently, the suspension was centrifuged at 3000 rpm (2682*g*) for 30 min, and the supernatant and residue were collected, respectively. This process was repeated for 20 times, and the first six batches of suspensions were mixed for HA extraction. The pH of the mixed supernatant was adjusted to 1 by adding 6 M HCl to make HA precipitate, and then, HA sample was separated by centrifugation. The HA was redissolved by adding 0.1 M KOH/0.3 M KCl under N_2, and then centrifuged to remove the suspended solids. HA was reprecipitated by adding 6 M HCl to adjust pH to 1, and the HA precipitate was suspended in 0.1 M HCl/0.3 M HF solution in a plastic container and shaken overnight at 50 °C. The residue (HM) was deashed with 0.1 M HCl/0.3 M HF solution for 10 times. HA and HM were transferred to dialysis tubes (Viskase Co., 3500 Da) by slurring with water and dialyze against distilled water until the dialysis water gives a negative Cl^- test with $AgNO_3$. Both HA and HM were freeze-dried, ground gently to pass through 100-mesh sieve, and stored in sealed brown glass bottles before usage.

The C, H, N contents of all samples were analyzed with high-temperature combustion method (PE 2400 SERIES II analyzer, Pekin-Elmer, Inc.), and O content was calculated by the mass difference. The ash content of samples was determined by heating at 750 °C for 5 h using muffle furnace. The content of acidic functional groups was determined by a titration method described in details elsewhere (Li et al. 2008). Solid-state cross-polarization magic angle spinning ^{13}C nuclear magnetic resonance (solid-state ^{13}C CP/MAS NMR) spectra of the samples were collected on a Bruker AVANCE III 400 NMR spectrometer with 4 mm NMR rotors with Kel-F caps. NMR spectra were obtained by applying the following parameters: rotor spin rate of 13 kHz, 1 s recycle time, 2 ms contact time, 20 ms acquisition time, and 10,000 scans. Chemical shifts were calibrated with adamantane.

Cr(VI) adsorption experiment

A series of 250 ml of Cr(VI) solutions with initial concentration of 5 mM were added into 300-ml brown flasks containing 125.0 ± 0.5 mg HA or HM. The solution contained a background electrolyte of 0.01 M NaCl, and the initial pH was adjusted to 1.0 by 2.5 M HCl. For complete mixing, each sample was shaken at 25 °C using an incubator shaker with the agitation of 200 rpm, and all experiments were performed in triplicate. At given time intervals, a batch of flasks were taken out, and then, vacuum filtration with 0.45 μm membrane was used to separate all undissolved HA and HM from the suspensions. The concentration of Cr(VI) in the filtrate was determined using a UV/Vis spectrophotometer (SHIMADZU UV-1800) at 540 nm after reacting with 1,5-diphenylcarbazide (DPC) (Hsu et al. 2010). The separated HA and HM samples (4 and 60 days) were freeze-dried, and then characterized by X-ray photoelectron spectroscopy (XPS), Fourier transform infrared spectroscopy (FTIR), and solid-state ^{13}C CP/MAS NMR.

XPS characterization

XPS was measured with Thermo escalab 250XI. The X-ray excitation was provided by a monochromatic Al Kα (excitation energy 1486.6 eV). The binding energies of the spectra were corrected using the hydrocarbon component of adventitious carbon at 284.8 eV.

FTIR characterization

FTIR spectra of samples were obtained on an IR spectrometer (Bruker LUMOS, Germany) at room temperature. All samples were fully ground to guarantee high homogeneity prior to tests. The samples were uniformly mixed with dried KBr powder at mass ratio of 1:200. Each spectrum was obtained after 64 scans with 2-cm^{-1} resolution.

The XPS data fitting was conducted on XPSPEAK 41 software. The FTIR data were normalized and denoised by Savitzky-Golay smoothing before analysis. The data treatment and plot drawing were performed using Excel 2013 and Origin 2016 software, respectively.

Results and discussion

Physicochemical properties of HA and HM

The physicochemical properties of HA and HM, including bulk element composition, acidic functional group content, and integrated ^{13}C CP/MAS NMR data are summarized in Table 2. The ash content of HM was much higher than that of HA, because HM was considered to be tightly bound to

Table 2 Bulk elemental composition, atomic ratios, acidic functional groups, and integrated solid-state ^{13}C CP/MAS data of HA and HM

Samples	Bulk elemental composition (wt%)				(N + O)/C[a]	Ash content (%)	-COOH content (mmol/g)	-OH content (mmol/g)
	C	H	O	N				
HA	57.21	5.63	31.23	3.61	0.46	1.01	2.89	3.56
HM	45.68	4.20	27.80	1.03	0.48	20.86	1.01	1.00
Samples	Chemical shift (ppm) and carbon assignment (%)					Aliphatic C (%)[b]	Polar C (%)[c]	Aromatic polar C (%)[d]
	0–50	50–112	112–145	145–163	163–190			
	Alkyl	O-alkyl	Aromatic	Phenolic	Carboxylic			
HA	41.68	17.42	17.58	7.23	16.09	59.10	40.74	23.32
HM	46.24	25.74	14.39	4.90	8.73	71.98	39.37	13.63

[a] (N + O)/C: atomic ratio of sum of nitrogen and oxygen to carbon

[b] Aliphatic C (%): total aliphatic C region (0–110 ppm)

[c] Polar C (%): total polar carbon region (50–110 and 145–200 ppm)

[d] Aromatic polar C (%): total polar carbon region (145–200 ppm)

minerals, and very difficult to separate from soil matrix result from the non-water-soluble property. According to the bulk elemental composition and element ratio of HA and HM, it can be found that their (N + O)/C value was comparable, which indicated that they had nearly the same content of polar C. However, the content of acidic functional groups for HA and HM determined by the titration method was quite different from each other, even though their contents of polar C were comparable. The carboxyl and phenol contents for HA were 2.89 and 3.56 mmol/g, respectively, and that for HM was only 1.01 and 1.00 mmol/g, and this indicated that HM tends to contain more apolar oxygen-containing functional groups than HA, such as ether, ester, and carbonyl, which is in good agreement with its hydrophobic property (Kang et al. 2003; Wang et al. 2011). Solid-state ^{13}C CP/MAS NMR was utilized to determine the C type distributions of HA and HM, and it was found that HM was more aliphatic compared with HA, and the polar C contents of HA and HM were similar with each other, coinciding with the result obtained from the value of (N + O)/C. The aromatic polar C content of HA, mainly carboxyl and phenol, was much higher than that of HM, which is in accordance with the results obtained from the titration experiment.

Cr(VI) adsorption by HA and HM

The variations of Cr concentration in solution induced by reacting with HA and HM are shown in Fig. 1. As indicated, the attenuation of Cr(VI) concentration in solution induced by reacting with HA was much more efficient than that with HM, and the attenuation rates were both rapid at the beginning stage (stage 1, 0–4 days) and much slower in the following stage (stage 2, 4–60 days). The change of the reaction rate was probably due to the fact that different mechanisms were in charge of the two stages. According to previous studies, Cr(VI) retention by undissolved HA was considered to follow an adsorption-reduction mechanism, where Cr(VI) is adsorbed onto HA surface through electrostatic attraction or ion exchange followed by the reduction of HA-bounded Cr(VI) to Cr(III) by adjacent functional groups, and then reduced Cr(III) may remain on the sorbent surface through complexation or be released into solution (Hsu et al. 2009; Janos et al. 2009; Zhang et al. 2017a, b). As shown in Fig. 1, the concentration of Cr(T) in solution for both HA and HM decreased simultaneously with Cr(VI) in stage 1, and this indicated that the decrease of Cr(VI) concentration in solution was mainly induced by Cr(VI) adsorption from aqueous phase onto HA and HM solid phase. In stage 2, Cr(T) concentration kept almost constant, even though the concentration of Cr(VI) in solution still decreased with time significantly. This indicated that Cr(VI) was continuously reduced to Cr(III), but nearly all reduced Cr(III) was released into the solution. According to the TOC analysis, less than 2% of HA and HM were dissolved in the solution throughout the experiment due to the low pH condition (the results were not shown), so the reduction of

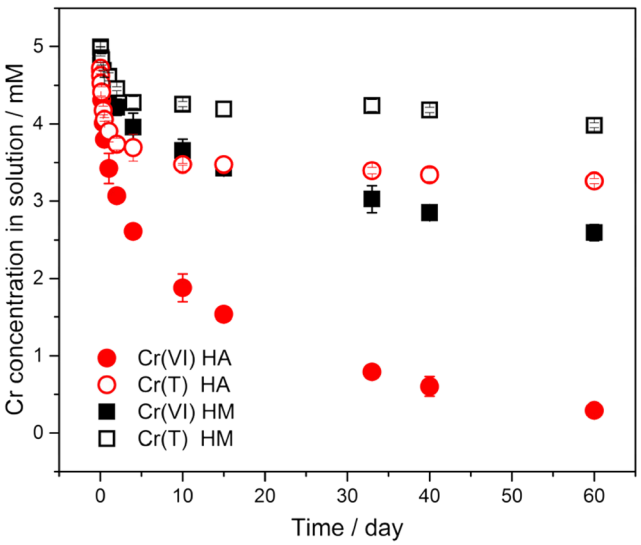

Fig. 1 Adsorption of 5 mM Cr(VI) by HA by HA and HM under pH 1.0 at 25 °C over 60 days. Error bars are SEM ($n = 3$)

Cr(VI) in solution can be neglected. Therefore, the release of Cr(III) may be mainly due to the fact that the complexation sites on HA and HM were saturated by Cr binding.

The increase of Cr(III) concentration in solution that was determined by the difference between Cr(T) and Cr(VI) concentration indicated that Cr(VI) was indeed reduced by HA and HM; however, it is still unclear whether all the Cr(VI) adsorbed onto HA and HM was reduced to Cr(III). To clarify Cr(VI) reduction extent on HA and HM, XPS Cr2p was employed to determine the oxidation state transformation of Cr with time on HA and HM surfaces, and the results are shown in Fig. 2. As indicated, by the end of stage 1 (4 days), there was still certain amount of Cr(VI) existing on HA and HM surfaces that has not been reduced to Cr(III), and it is probably due to the fact that the rate of Cr(VI) adsorption was much faster than that of Cr(VI) reduction resulting in the accumulation of Cr(VI) on HA and HM surfaces. However, by the end of stage 2 (60 days), there was no Cr(VI) to be detected. The reason may be that Cr(VI) concentration in bulk solution decreased significantly resulting in the decreasing reaction rate of Cr(VI) adsorption onto HA and HM, and thus, Cr(VI) reduction process was not the rate-limiting step any more, resulting in the decreasing of Cr(VI) percentage on HA and HM. According to the results above, it can be concluded that Cr(VI) reduction indeed occurred on HA and HM surfaces.

Roles of HA and HM functional groups

As the primary electron donors for Cr(VI) reduction, the variations of HA and HM functional groups were regarded as the most important point for understanding their interaction mechanism, and FTIR spectra from 1750 to 950 cm^{-1} were utilized to determine HA and HM functional groups changing during reaction with Cr(VI) as shown in Fig. 3. The absorbance peaks at 1708, 1626, 1226, and 1078 cm^{-1} for HA and HM both decreased significantly with time, which were, respectively, assigned to C=O stretching vibration of carboxyl, C=O stretching vibration of carbonyl, the C–O stretching vibration of phenol, and C–O stretching vibration of hydroxyl (Fanning and Vannice 1993; Li et al. 2003; O'Reilly and Mosher 1983; Sellitti et al. 1990). This indicated that these functional groups were very likely involved in the reaction with Cr(VI), but it was still unclear whether they were all oxidized by Cr(VI). As shown in Fig. 3, the absorbance peak at 1555 cm^{-1} for HA and HM both increased significantly with time, which was attributed to the stretching vibration of chelated carboxyl (Zhao et al. 2016). This indicated that the Cr was fixed on HA and HM surfaces though complexation with carboxylic groups. Since FTIR peak intensity variation cannot only be effected by oxidation process, where one kind of functional group can be transformed into another type, but the complexation can also induce red or blue shift of FITR peak position, which

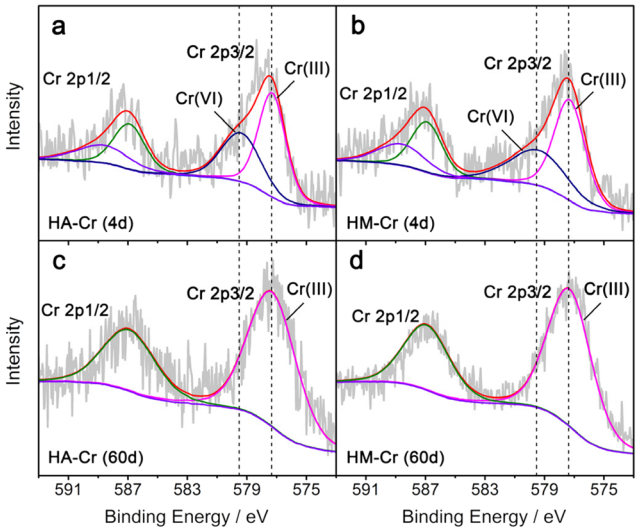

Fig. 2 XPS Cr2p spectra of HA and HM samples after reacting with 5 mM Cr(VI) under pH 1.0 at 25 °C for 4 and 60 days. The peaks at 588.7 and 586.9 eV were assigned to $Cr2p_{1/2}$ of Cr(VI) and Cr(III). The peaks at 579.4 and 577.3 eV were assigned to $Cr2p_{3/2}$ of Cr(VI) and Cr(III)

means whether these functional groups participated in the reduction of Cr(VI) or otherwise cannot be determined by FTIR spectra alone. However, at least, it can be concluded that mainly carboxyl, carbonyl, phenol, and hydroxyl took part in the reaction with Cr(VI).

Since FTIR is a type of molecular spectroscopy, the complex of functional groups with Cr will dramatically change its molecular orbital configuration resulting in significant change of FITR peak intensity. However, XPS is a type of electron spectroscopy, especially for the inner electron, and the excitation energy of inner orbital electron will not be greatly

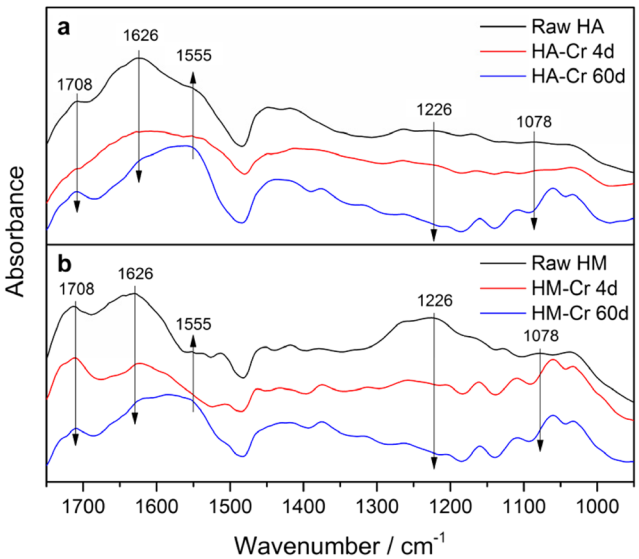

Fig. 3 FTIR spectra of **a** HA and **b** HM samples after reacting with 5 mM Cr(VI) under pH 1.0 at 25 °C for 4 and 60 days. The raw HA and HM are referring to the samples without any perturbation

influenced by outer valence electron participating in complex reaction. Therefore, XPS C1s spectra were employed to determine whether all the functional groups mentioned above participated in the reduction of Cr(VI), and the results are shown in Fig. 4. As shown, the XPS peaks for HA and HM at 284.8, 287.1, and 288.7 eV, which were attributed to C–H or C–C, C=O, and O–C=O, respectively, all remained nearly unchanged from 4 to 60 days. However, the XPS peaks for HA and HM at 286.1 eV assigned to C–O both decreased significantly from 4 to 60 days, which indicated that C–O involved in the functional groups of phenol and hydroxyl on the surfaces of HA and HM was almost thoroughly eliminated resulting from oxidation by Cr(VI). On the contrary, the resistance of C–H, C–C, C=O, and O–C=O on the surfaces of HA and HM indicated that aliphatic hydrocarbon, carbonyl, and carboxyl groups did not tend to be oxidized by Cr(VI), and the decreasing FTIR absorbance of carboxyl and carbonyl for HA and HM were more likely induced by the complexation with Cr.

In addition, it should be pointed out that the detection depth of XPS is quite different from FTIR test, which can only collect the signals within few-nanometer depth on particle surfaces instead of the whole sample, and thus the undetectable C–O peaks of HA and HM after reacting with Cr(VI) for 60 days tended to be induced by the oxidation of C–O-related functional groups on the particle surfaces instead of in the bulk samples. Furthermore, the FTIR absorbance peaks of HA and HM that ranged from 1000 to 1200 cm^{-1}, attributed to the C–O stretching vibration of hydroxyl and ether, were still significant after reacting with Cr(VI) for 60 days, and this indicated the existence of oxygen containing functional groups in the bulk samples by the end of experiment. Therefore, it can be drawn from these two opposite phenomena that C–O-related functional groups (such as phenol, hydroxyl, and ether) on the surface of HA and HM were more active than that in their interior part.

Solid-state ^{13}C CP/MAS NMR was employed to reveal the variations of HA and HM molecular structure after reacting with Cr(VI). As shown in Fig. 5a, b, the NMR spectra of HA and HM are quite different from each other, and this demonstrates that they are two different typical fractions of soil humus with distinct molecular structures. The NMR spectral shapes are quite similar with corresponding fraction extracted from the peat soils purchased from the IHSS that has been reported previously (Bonin and Simpson 2007), but the aliphaticity of the samples used in this study is comparatively higher. As indicated, the NMR peaks of HA and HM in the range from 0 to 50 ppm remained approximately unchanged during reacting with Cr(VI), which are attributed to alkyl C, and this indicated that the aliphatic structures of HA and HM were both resistant to the oxidiction of Cr(VI). On the other hand, the NMR peaks of HA and HM at 130 and 154 ppm both decreased significantly after reacting with Cr(VI), which were, respectively, assigned to aromatic C and phenol C (Xing 2001), and this indicated that both the aromatic C and phenol C of HA and HM tended to participate in the reaction with Cr(VI). On the contrary, the variations of O-alkyl C (50–110 ppm) and carboxyl C (163–185 ppm) for HA and HM were quite different from each other, especially for the O-alkyl C. It can be seen that the peaks of HA and HM at 56 and

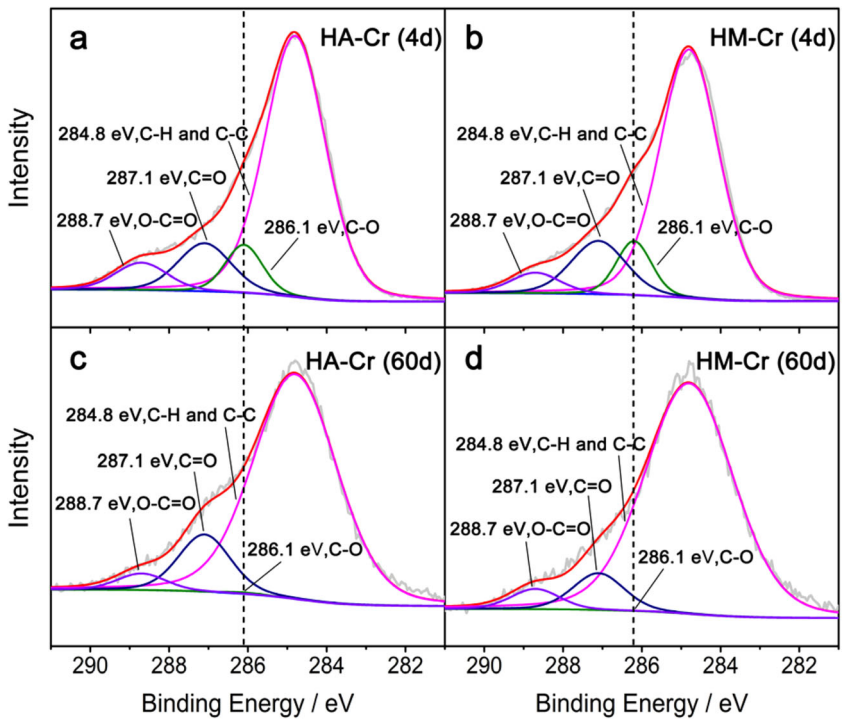

Fig. 4 XPS C1s spectra of HA and HM samples after reacting with 5 mM Cr(VI) under pH 1.0 at 25 °C for 4 and 60 days

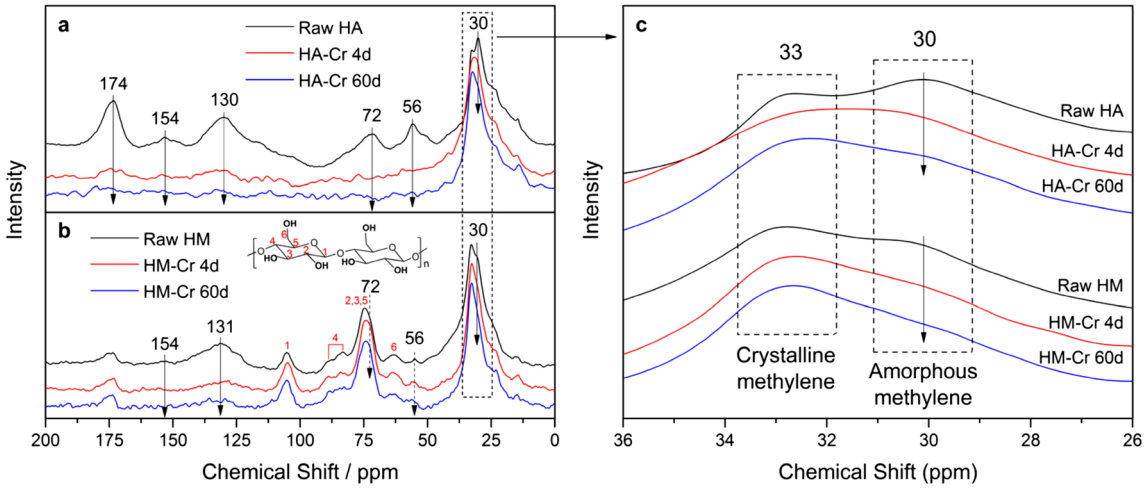

Fig. 5 Solid-state ^{13}C CP/MAS NMR spectra of HA and HM samples after reacting with 5 mM Cr(VI) under pH 1.0 at 25 °C for 4 and 60 days. The assignments of different chemical shift ranges are shown as following: alkyl C (0–50 ppm), O-alkyl C (50–110 ppm), aromatic C (110–145 ppm), phenol C (145–163 ppm), and carboxyl C (163–185 ppm). The raw HA and HM are referring to the samples without any perturbation

72 ppm decreased with various extent after reacting with Cr(VI), which are assigned to methoxyl and secondary alcohol, respectively, and this implies that these two oxygen-containing functional groups of HA and HM are readily to be oxidized by Cr(VI). However, the peaks of HM at 63, 74, 83, 89, and 105 ppm remained almost unchanged, which can be attributed to the carbons in the ring structure of cellulose (Vanderhart and Atalla 1984; Wang and Hong 2015), and this indicated that HM has a high content of cellulose, and the cellulose structures are quite resistant to Cr(VI) oxidation, which can be responsible for the low efficiency of Cr(VI) reduction by HM. Additionally, it can be seen from Fig. 5c that the peaks of HA and HM at 30 ppm decreased significantly, but the peaks at 33 ppm kept almost unchanged. The doublet peaks at 30 and 33 ppm can be assigned to amorphous and crystalline methylene, respectively, and the crystalline methylene carbon is suggested to be resistant to environmental attack, but the amorphous one not (Weiguo Hu et al. 2016). The crystalline methylene carbon proportion of raw HM is much higher than that of raw HA, and this may partially account for the lower capability of HM for Cr(VI) reduction as well.

Conclusion

In this work, the molecular characteristics and reduction capability for Cr(VI) by HA and HM fractions of a black soil from Northeast China were investigated, and the mechanism of HA and HM functional groups for Cr(VI) reduction was revealed. Phenol and hydroxyl were determined as the main electron donors for Cr(VI) reduction by HA and HM rather than carboxyl and carbonyl, which were more likely involved in the complexation with Cr. Furthermore, phenol and hydroxyl on the particle surfaces of HA and HM were much more active on Cr(VI) reduction than that in their interior part. However, HM was found to be more aliphatic than HA with a higher content of cellulose structures, which were found to be quite resistant to the oxidation of Cr(VI) resulting in the lower capability of HM for Cr(VI) reduction. These results suggest that in soil environment, undissolved HA tends to play a much more important role compared with HM in Cr(VI) reduction and retention in the condition that their mass contents are comparable. Additionally, the quantitive relationship between Cr(VI) reduction rate and the contents of functional groups that act as electron donors can be another issue of great concerns, which can be the next move of efforts on this topic.

Acknowledgements This work was financially supported by the National Natural Science Foundation of China (Grant 41672239) and China Geological Survey (1212011121173).

References

Al-Abadleh HA, Mifflin AL, Bertin PA, Nguyen ST, Geiger FM (2005) Control of carboxylic acid and ester groups on chromium (VI) binding to functionalized silica/water interfaces studied by second harmonic generation. J Phys Chem B 109:9691–9702. https://doi.org/10.1021/jp050782o

Bonin JL, Simpson MJ (2007) Variation in phenanthrene sorption coefficients with soil organic matter fractionation: the result of structure or conformation? Environ Sci Technol 41:153–159. https://doi.org/10.1021/es061471+

Brose DA, James BR (2010) Oxidation-reduction transformations of chromium in aerobic soils and the role of electron-shuttling quinones. Environ Sci Technol 44:9438–9444. https://doi.org/10.1021/es101859b

Dermentzis K, Christoforidis A, Valsamidou E, Lazaridou A, Kokkinos N (2011) Removal of hexavalent chromium from electroplating

wastewater by electrocoagulation with iron electrodes. Global Nest J 13:412–418

Dhal B, Thatoi HN, Das NN, Pandey BD (2013) Chemical and microbial remediation of hexavalent chromium from contaminated soil and mining/metallurgical solid waste: a review. J Hazard Mater 250-251C:272–291. https://doi.org/10.1016/j.jhazmat.2013.01.048

Fanning PE, Vannice MA (1993) A drifts study of the formation of surface groups on carbon by oxidation. Carbon 31:721–730. https://doi.org/10.1016/0008-6223(93)90009-Y

Fendorf SE (1995) Surface reactions of chromium in soils and waters. Geoderma 67:55–71. https://doi.org/10.1016/0016-7061(94)00062-F

Hsu CL, Wang SL, Tzou YM (2007) Photocatalytic reduction of Cr(VI) in the presence of NO3- and cl- electrolytes as influenced by Fe(III). Environ Sci Technol 41:7907–7914. https://doi.org/10.1021/es0718164

Hsu NH, Wang SL, Lin YC, Sheng GD, Lee JF (2009) Reduction of Cr(VI) by crop-residue-derived black carbon. Environ Sci Technol 43:8801–8806. https://doi.org/10.1021/es901872x

Hsu LC, Wang SL, Lin YC, Wang MK, Chiang PN, Liu JC, Kuan WH, Chen CC, Tzou YM (2010) Cr(VI) removal on fungal biomass of Neurospora crassa: the importance of dissolved organic carbons derived from the biomass to Cr(VI) reduction. Environ Sci Technol 44:6202–6208. https://doi.org/10.1021/es1017015

Hu W, Mao J, Baoshan Xing A, Schmidtrohr K (2016) Poly(methylene) Crystallites in Humic Substances Detected by Nuclear Magnetic Resonance. Environ Sci Technol 34:530–534. https://doi.org/10.1021/es9905061

Janos P, Hula V, Bradnova P, Pilarova V, Sedlbauer J (2009) Reduction and immobilization of hexavalent chromium with coal- and humate-based sorbents. Chemosphere 75:732–738. https://doi.org/10.1016/j.chemosphere.2009.01.037

Jardine PM, Fendorf SE, Mayes MA, Larsen IL, Brooks SC, Bailey WB (1999) Fate and transport of hexavalent chromium in undisturbed heterogeneous soil. Environ Sci Technol 33:2939–2944. https://doi.org/10.1021/es981211v

Kang S, Amarasiriwardena D, Veneman P, Xing (2003) Characterization of ten sequentially extracted humic acids and a humin from a soil in western Massachusetts. Soil Sci 168:880–887. https://doi.org/10.1097/01.ss.0000106404.84926.b0

Kimbrough DE, Cohen Y, Winer AM, Creelman L, Mabuni C (1999) A critical assessment of chromium in the environment. C R C. Crit Rev Environ Control 29:1–46. https://doi.org/10.1080/10643389991259164

Kožuh N, Štupar J, Gorenc B (2000) Reduction and oxidation processes of chromium in soils. Environ Sci Technol 34:112–119. https://doi.org/10.1021/es981162m

Li L, Huang W, Peng PA, Sheng G, Fu J (2003) Chemical and molecular heterogeneity of humic acids repetitively extracted from a peat. Soil Sci Soc Am J 67:740–746. https://doi.org/10.2136/sssaj2003.0740

Li Y, Yue Q, Gao B, Li Q, Li C (2008) Adsorption thermodynamic and kinetic studies of dissolved chromium onto humic acids. Colloids Surfaces B Biointerfaces 65:25–29. https://doi.org/10.1016/j.colsurfb.2008.02.014

Liu J, Zhang XH, Tran H, Wang DQ, Zhu YN (2011) Heavy metal contamination and risk assessment in water, paddy soil, and rice around an electroplating plant. Environ Sci Pollut Res 18:1623–1632. https://doi.org/10.1007/s11356-011-0523-3

Nickens KP, Patierno SR, Ceryak S (2010) Chromium genotoxicity: a double-edged sword. Chem Biol Interact 188:276–288. https://doi.org/10.1016/j.cbi.2010.04.018

O'Reilly JM, Mosher RA (1983) Functional groups in carbon black by FTIR spectroscopy. Carbon 21:47–51. https://doi.org/10.1016/0008-6223(83)90155-0

Raddatz AL, Johnson TM, Mcling TL (2011) Cr stable isotopes in Snake River plain aquifer groundwater: evidence for natural reduction of dissolved Cr(VI). Environ Sci Technol 45:502–507. https://doi.org/10.1021/es102000z

Sellitti C, Koenig JL, Ishida H (1990) Surface characterization of graphitized carbon-fibers by attenuated total reflection fourier-transform infrared-spectroscopy. Carbon 28:221–228. https://doi.org/10.1016/0008-6223(90)90116-G

Simpson AJ, Song G, Smith E, Lam B, Novotny EH, Hayes MH (2007) Unraveling the structural components of soil humin by use of solution-state nuclear magnetic resonance spectroscopy. Environ Sci Technol 41:876–883. https://doi.org/10.1021/es071217x

Tang J, Petersen E, Weber WJ (2008) Development of engineered natural organic sorbents for environmental applications. 4. Effects on biodegradation and distribution of pyrene in soils. Environ Sci Technol 42: 1283–1289. https://doi.org/10.1021/es071999u

Van ZA, Comans RN (2007) Measurement of humic and fulvic acid concentrations and dissolution properties by a rapid batch procedure. Environ Sci Technol 41:6755–6761. https://doi.org/10.1021/es0709223

Vanderhart DL, Atalla RH (1984) Studies of microstructure in native celluloses using solid-state carbon-13 NMR. Macromolecules 17: 1465–1472. https://doi.org/10.1021/ma00138a009

Wang T, Hong M (2015) Solid-state NMR investigations of cellulose structure and interactions with matrix polysaccharides in plant primary cell walls. J Exp Bot 20:333–338. https://doi.org/10.1093/jxb/erv416

Wang X, Guo X, Yang Y, Tao S, Xing B (2011) Sorption mechanisms of phenanthrene, lindane, and atrazine with various humic acid fractions from a single soil sample. Environ Sci Technol 45:2124–2130. https://doi.org/10.1021/es102468z

Watanabe A, Kuwatsuka S (1991) Triangular diagram for humus composition in various types of soils. Soil Sci Plant Nutrition 37:167–170. https://doi.org/10.1080/00380768.1991.10415023

Wittbrodt PR, Palmer CD (1996) Effect of temperature, ionic strength, background electrolytes, and Fe(III) on the reduction of hexavalent chromium by soil humic substances. Environ Sci Technol 30:2470–2477. https://doi.org/10.1021/es950731c

Xiao W, Zhang Y, Li T, Chen B, Wang H, He Z, Yang X (2012) Reduction kinetics of hexavalent chromium in soils and its correlation with soil properties. J Environ Qual 41:1452–1458. https://doi.org/10.2134/jeq2012.0061

Xing B (2001) Sorption of naphthalene and phenanthrene by soil humic acids. Environ Pollut 111:303–309. https://doi.org/10.1016/S0269-7491(00)00065-8

Yang Y, Shu L, Wang X, Xing B, Tao S (2011) Impact of de-ashing humic acid and humin on organic matter structural properties and sorption mechanisms of phenanthrene. Environ Sci Technol 45:3996–4002. https://doi.org/10.1021/es2003149

Zhang JH, He MC, Shi YH (2009a) Comparative sorption of benzo[α]phrene to different humic acids and humin in sediments. J Hazard Mater 166:802–809. https://doi.org/10.1016/j.jhazmat.2008.11.121

Zhang JJ, Dou S, Song XY (2009b) Effect of long-term combined nitrogen and phosphorus fertilizer application on ^{13}C CPMAS NMR spectra of humin in a Typic hapludoll of Northeast China. Eur J Soil Sci 60:966–973. https://doi.org/10.1111/j.1365-2389.2009.01191.x

Zhang J, Wang S, Wang Q, Wang N, Li C, Wang L (2013) First determination of cu adsorption on soil humin. Environ Chem Lett 11:41–46. https://doi.org/10.1007/s10311-012-0375-1

Zhang J, Chen L, Yin H, Jin S, Liu F, Chen H (2017a) Mechanism study of humic acid functional groups for Cr(VI) retention: two-dimensional FTIR and (13)C CP/MAS NMR correlation spectroscopic analysis. Environ Pollut 225:86–92. https://doi.org/10.1016/j.envpol.2017.03.047

Zhang J, Yin H, Chen L, Liu F, Chen H (2017b) The role of different functional groups in a novel adsorption-complexation-reduction

multi-step kinetic model for hexavalent chromium retention by undissolved humic acid. Environ Pollut. https://doi.org/10.1016/j.envpol.2017.10.120

Zhang J, Yin H, Samuel B, Liu F, Chen H (2018) A novel method of three-dimensional hetero-spectral correlation analysis for the fingerprint identification of humic acid functional groups for hexavalent chromium retention. RSC Adv 8:3522–3529. https://doi.org/10.1039/C7RA12146F

Zhao TT, Ge WZ, Nie YX, Wang YX, Zeng FG, Qiao Y (2016) Highly efficient detoxification of Cr(VI) by brown coal and kerogen: process and structure studies. Fuel Process Technol 150:71–77. https://doi.org/10.1016/j.fuproc.2016.05.001